InP Photonic Integrated Circuit with an AWG-like design for Optical Beam Steering

Weihua Guo[1], Pietro R. A. Binetti[1], Chad Althouse[1], Huub P.M.M. Ambrosius[2], Leif A. Johansson[1], member, IEEE, and Larry A. Coldren[1], Fellow, IEEE

[1]*Department of Electrical and Computer Engineering, University of California Santa Barbara, CA93106, USA*

[2]*Electrical Engineering Department, Eindhoven University of Technology, Eindhoven, NL*

***Abstract* — Optical beam steering through an InP PIC with an AWG-like design has been demonstrated. Good far-field pattern has been kept without resetting the phase shifter currents when changing the input wavelength to steer the beam.**

***Index Terms* — Photonic integrated circuits, optical beam steering, LIDAR.**

I. Introduction

Similar to electronically scanned phased array Radar, electronically controlled optical beam steering is useful for light detecting and ranging (LIDAR). It also finds applications in 3D imaging, precision targeting, guidance and navigation, etc. Different methods have been tried to achieve electronically controlled optical beam steering [1-3]. In [4-5] we demonstrated electronically controlled 2D optical beam steering through an InP photonic integrated circuit (PIC). The critical part of the PIC is a waveguide array with embedded 2nd-order gratings for out-of-plane emission. An array of phase shifters is used to add a phase slope across the waveguide array so as to steer the beam perpendicularly to the waveguide in the array (lateral direction) [4]. The input wavelength is changed to steer the beam along the waveguide in the array (longitudinal direction) because the emission angle of the grating depends on wavelength [4]. Because of phase errors caused by imperfect fabrication, we normally need to optimize the phase shifter currents to generate a good beam—narrow beam width and high side-lobe suppression for the far-field pattern. Because it is a 2D scan it would be preferable not to reset the phase shifter currents when changing wavelength. In this work, we show that through an AWG-like design, i.e. all the channels use bends with the same radius and the same length, the far-field pattern of the beam can keep a good shape and high side-lobe suppression when changing the input wavelength even when we do not reset the phased shifter currents.

II. PIC LAYOUT

The PIC layout is shown in Fig. 1. After amplification by a preamplifier—the leftmost semiconductor optical amplifier (SOA), the input signal is split into eight channels by a 1×8 splitter consisting of cascaded 1×2 MMIs. Each channel then has its own SOA and phase shifter to boost the power and control the phase. After passing through some additional waveguides consisting mostly of bends with the same radius and the same total bending angles (1.5π), the signal enters into the waveguide array region as shown in Fig. 1.

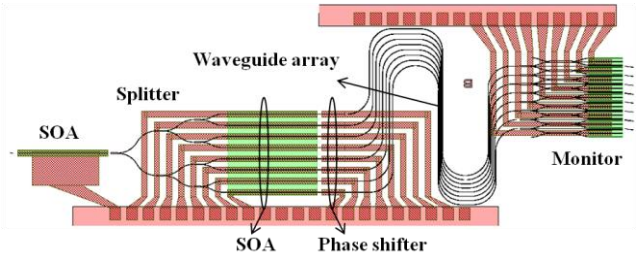

Fig. 1. Layout of the PIC.

Each waveguide in the waveguide array is passive and has embedded 2nd-order gratings etched into the upper optical confinement layer of the waveguide core and buried by the regrown P-doped cladding layers. These gratings scatter the signal from the waveguide out of the plane, upward and downward. There is an aperture in the N-contact metal which is on the backside of the thinned-down substrate. This aperture is aligned to the gratings so that the downward emission can transmit through and be detected in our measurement setup. The additional bending waveguides are added to make all the channels have the same length from the end of the phase shifters to the beginning of the 2nd-order gratings. They are needed because the spacing between the SOA array and the waveguide array for emission is different: the former is 100 μm but the latter is only 5.5 μm. After passing through the waveguide array for emission, some signal which is still left in the waveguide passes through additional bending waveguides and then enters into the monitor array. These additional bending waveguides are needed due to the same reason as those added before the grating array. The monitors integrated on chip are used to monitor the phase difference between adjacent channels through interferometer structures formed by adjacent channels. All waveguides used in the PIC including both active and passive waveguides are deep ridge waveguides which allow small bend radius—200 μm—to be used. Because

of the relatively long bends and the tight bend radius, it is better to use the same bend radius and the same total bend length in each channel so that their influence on phase can cancel each other. This is a rule quite generally followed by AWG designs especially when waveguides with strong optical confinement are used [6].

III. PIC FABRICATION

The PIC as being introduced in the above section includes both passive and active waveguides. The active-passive integration has been realized by using the quantum well intermixing technique [7-8]. Starting from a base wafer structure as shown in Fig. 2 (a), phosphorous ions are implanted into the top sacrificial InP layer to produce defects in the area intended to be passive. These defects are then thermally driven down through the quantum well layers to cause component mixture between the barrier and well materials. This is the so-called quantum well intermixing process which increases the bandgap of the quantum wells in the implanted area. After intermixing, the top InP sacrificial layer is removed by wet etching then the 2nd-order gratings are patterned by using electron beam lithography and etched into the upper optical confinement layer of the waveguide core. After that a P-doped InP cladding layer is re-grown above followed by the highly P-doped InGaAs contact layer. The full wafer structure after regrowth is schematically shown in Fig. 2 (b). The waveguides are patterned by using the I-line wafer stepper and are etched by using ICP with the $Cl_2/H_2/Ar$ plasma [9]. The etch depth is about 5 μm so all the waveguides including both active and passive waveguides are deeply etched ridge waveguides. After waveguide etching is the SiN_x isolation layer deposition followed by via opening for the P-metal and P-metal deposition. Then the wafer is thinned down and N-metal is put on the backside of the wafer. An aperture has been opened in the N-metal which is aligned to the grating area to allow the downward emission from the grating to transmit through.

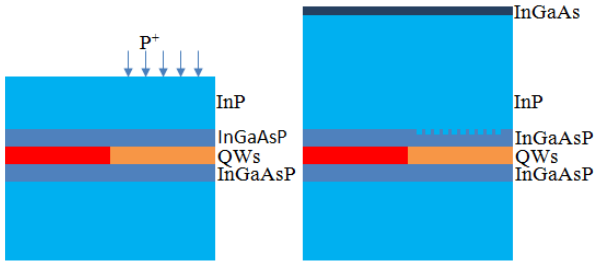

Fig. 2. Schematic wafer structure before regrowth (a) and after regrowth (b).

III. MEASUREMENT

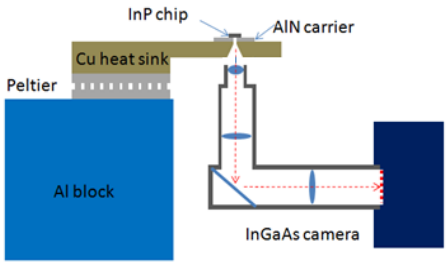

Fig. 3. Schematic of the measurement setup.

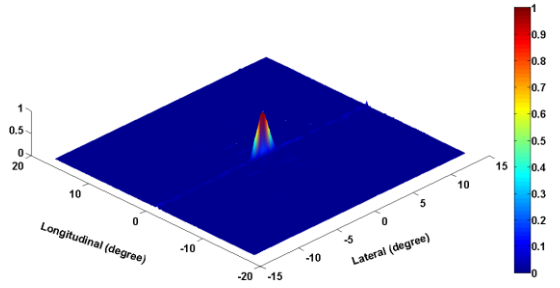

(a)

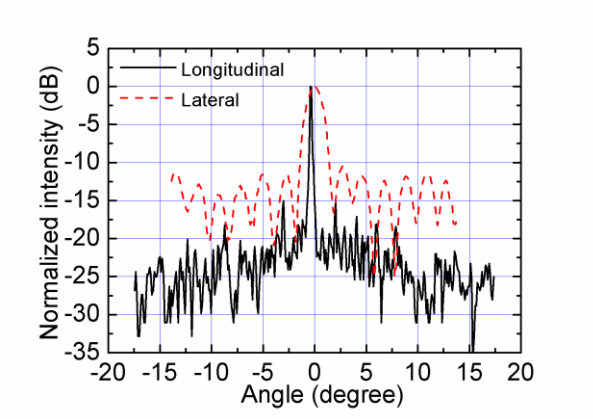

(b)

Fig. 4. (a) Far-field pattern when the beam pointing at zero degree in the lateral direction and the input wavelength is 1540 nm; (b) Intensity distribution across the peak in the lateral and longitudinal direction.

The measurement setup is schematically shown in Fig. 3. The PIC is mounted facing-up onto an AlN carrier. There are holes in the carrier and the Cu heat sink which are aligned to the aperture of the N-contact metal of the PIC so that the downward emission can be captured by the imaging system as shown in Fig. 3. The imaging system consists of three lenses with folded optical path and an InGaAs infrared camera. The first lens projects the far-field pattern of the emission onto its lower focal plane. The far-field pattern is then magnified and

projected onto the detector plane of the infrared camera by the other two lenses. The imaging system is able to capture the far-field from -17 to 17 degrees in the longitudinal direction and from -14 to 14 degrees in the lateral direction with an angle resolution of ~0.1 degree. For the following measurement the on-chip SOAs are all biased at 100 mA. The eight channel SOAs are biased by a single current source. To account for the series resistance difference of the SOAs, a variable resistor network has been used as demonstrated in [5]. The eight phase shifters are controlled by eight current analog outputs from a DAC card. The input signal is from an external cavity tunable laser fiber coupled into the chip. The tuning range is set from 1530 to 1560 nm.

First, the input wavelength is set to 1540 nm. The phase shifter currents are optimized by the Particle Swarm Optimization (PSO) algorithm to make the beam point at zero degree in the lateral direction and to maximize the side-lobe suppression ratio in the angle range from -14 to 14 degrees [4]. The resulted 2D far-field pattern is plotted in Fig. 4 (a) which shows that a nice clean beam has been obtained. The intensity distribution across the peak in the lateral and longitudinal direction is shown in Fig. 4 (b). A side-lobe suppression of 10 dB has been achieved. The 3-dB beam width in the lateral direction is 1.7 degrees which is in close agreement of the theoretical value of 1.8 degrees, assuming the emission amplitude is uniform across the eight channels. In the longitudinal direction the beam is much narrower because a very long (500 μm) and slowly attenuating grating has been used. Then, we steer the beam to different angles in the lateral direction by repeating the above optimization process around the lateral angles from -6 to 6 degrees with a step of 2 degrees. The results are shown in Fig. 5. The array spacing is 5.5 μm which determines that the angle spacing between two adjacent diffraction orders is 16 degrees, as it can be clearly seen from Fig. 5.

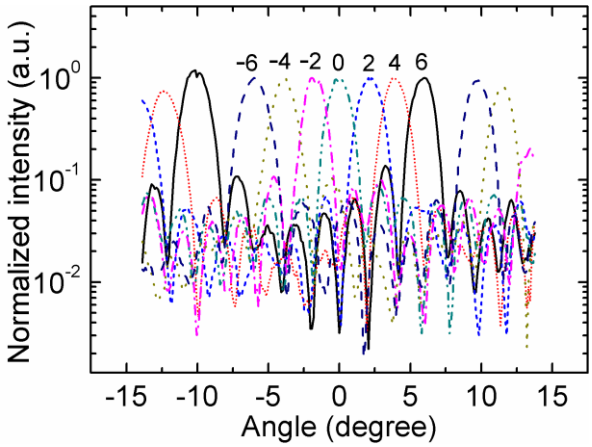

Fig. 5. Intensity distribution in the lateral direction when the beam steered to lateral angles from -6 to 6 degrees with a step of 2 degrees.

After this, we steered the beam back to the lateral zero-degree angle and then changed the wavelength from 1530 to 1560 nm. Without changing the phase shifter currents, the far-field pattern in the lateral direction is recorded and plotted in Fig. 6. When changing the wavelength, the gain of the SOAs on-chip varies due to the limited gain bandwidth and the fixed current injections to the SOAs. This influences the output power as seen from Fig. 6. But the 3-dB beam width and the side-lobe suppression keep nearly the same, ~2.0 degrees and 10 dB, respectively. For the wavelength of 1550 nm which is the gain peak, the emission is a little bit too strong to saturate the infrared camera which causes the peak of the recorded field distribution to be cut-off. The design not only keeps the length of all the channels the same but also uses the same bends: the same bend radius and the same total bending angles. Furthermore all the SOAs and phase shifters are arranged to have the same positions relative to the splitter and to the grating array. All of these help to achieve the effect shown in Fig. 6. But there is also one penalty from these additional waveguides—the added loss. Our passive waveguides typically have a loss of about 2 dB/mm. So these additional waveguides contribute to a loss of about 4 dB due to their ~2 mm length.

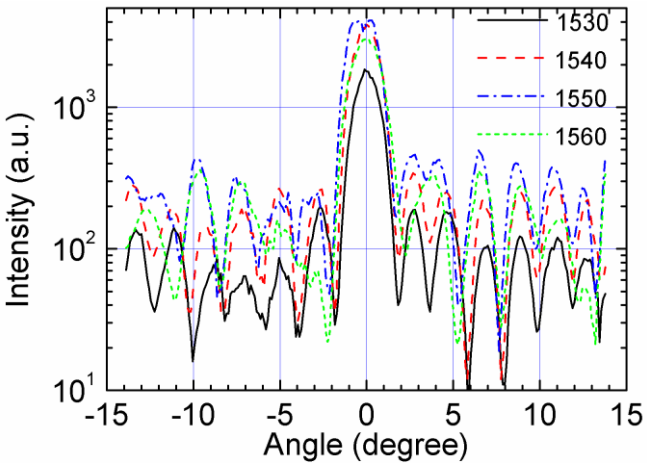

Fig. 6. Far-field pattern in the lateral direction for the input wavelength of 1530, 1540, 1550, and 1560 nm.

IV. Summary

In summary we have demonstrated an InP PIC for optical beam steering: when we change the input wavelength to steer the beam the array of phase shifters does not need to reset the bias currents in order to preserve the beam shape and the side-lobe suppression. The AWG-like design employed in the PIC uses bends with the same radius and the same total length in each channel. This ensures that the influences from these bends cancel with each other even when a very tight bend radius—200 μm—has been used.

ACKNOWLEDGEMENT

This work is supported by DARPA SWEEPER project.

REFERENCES

[1] D. P. Resler, D. S. Hobbs, R. C. Sharp, L. J. Friedman, and T. A. Dorschner, "High-efficiency liquid-crystal optical phased-array beam steering," *Opt. Lett.*, vol. 21, no. 9, pp. 689-691, May 1996.

[2] A. Tuantranont, V. M. Bright, J. Zhang, W. Zhang, J. A. Neff, Y. C. Lee, "Optical beam steering using MEMS-controllable microlens array," *Sens. Actuators A: Phys.*, vol. 91, no. 3, pp. 363-372, Jul. 2001.

[3] K. Van Acoleyen, W. Bogaerts, R. Baets, "Two-dimensional dispersive off-chip beam scanner fabricated on silicon-on-insulator," *IEEE Photon. Technol. Lett.*, vol. 23, no. 17, pp. 1270-1272, Sep. 2011.

[4] W. H. Guo, P. R. A. Binetti, C. Althouse, A. Bhardwaj, J. K. Doylend, H. P. M. M. Ambrosius, L. A. Johansson, and L. A. Coldren, "InP photonic integrated circuit for 2D optical beam steering," Post-deadline paper, IEEE Photonics 2011 (IPC11), Arlington, Virginia, USA, 2011.

[5] W. H. Guo, P. R. A. Binetti, C. Althouse, H. P. M. M. Ambrosius, L. A. Johansson, and L. A. Coldren, "Improved performance of optical beam steering through an InP photonic integrated circuit," CW1K, CLEO, San Jose, CA, USA, 2012.

[6] H. Takahashi, I. Nishi, and Y. Hibino, "10 GHz spacing optical frequency division multiplexer based on arrayed-waveguide grating," *Electron. Lett.,* vol 28, no. 4, pp. 380-382, Feb. 1992.

[7] E. J. Skogen, J. S. Barton, S. P. Denbaars, and L. A. Coldren, "A quantum-well-intermixing process for wavelength-agile photonic integrated circuits," *IEEE J. Select. Topics Quantum Electron.*, vol. 8, no. 4, pp. 863-869, Jul./Aug. 2002.

[8] P. R. A. Binetti, M. Z. Lu, E. J. Norberg, R. S. Guzzon, J. S. Parker, A. Sivananthan, A. Bhardwaj, L. A. Johansson, M. J. Rodwell, and L. A. Coldren, "Indium phosphide photonic integrated circuits for coherent optical links," *IEEE J. Select. Topics Quantum Electron.*, vol. 48, no. 2, pp. 279-291, Feb. 2012.

[9] J. S. Parker, E. J. Norberg, R. S. Guzzon, S. C. Nicholes, and L. A. Coldren, "High verticality InP/InGaAsP etching in $Cl_2/H_2/Ar$ inductively coupled plasma for photonic integrated circuits," *J. Vac. Sci. Technol. B*, vol. 29, no. 1, Jan./Feb. 2011.